



## Virtual Knot Theory

LOUIS H. KAUFFMAN

This paper is an introduction to the theory of virtual knots. It is dedicated to the memory of Francois Jaeger.

© 1999 Academic Press

### 1. INTRODUCTION

This paper is an introduction to the subject of virtual knot theory, a generalization of classical knot theory that I discovered in 1996 [2]. This paper gives the basic definitions, some fundamental properties and a collection of examples. Subsequent papers will treat specific topics such as classical and quantum link invariants and Vassiliev invariants for virtual knots and links in more detail.

Throughout this paper I shall refer to knots and links by the generic term ‘knot’. In referring to a trivial fundamental group of a knot, I mean that the fundamental group is isomorphic to the integers.

The paper is organized as follows. Section 2 gives the definition of a virtual knot in terms of diagrams and moves on diagrams. Section 3 discusses both the motivation from knots in thickened surfaces and the abstract properties of Gauss codes. Section 3 proves basic results about virtual knots by using reconstruction properties of Gauss codes. In particular, we show how virtual knots can be identified as virtual by examining their codes. Section 4 discusses the fundamental group and the quandle extended for virtual knots. Examples are given of non-trivial virtual knots with a trivial (isomorphic to the integers) fundamental group. An example shows that some virtual knots are distinguished from their mirror images by the fundamental group, a very non-classical effect. Section 5 shows how the bracket polynomial (hence the Jones polynomial) extends naturally to virtuals and gives examples of non-trivial virtual knots with a trivial Jones polynomial. Examples of infinitely many distinct virtuals with the same fundamental group are verified by using the bracket polynomial. An example is given of a knotted virtual with a trivial fundamental group and unit Jones polynomial. It is conjectured that this phenomenon cannot happen with virtuals whose shadow code is classical. In Section 6 we show how to extend quantum link invariants and introduce the concept of virtual framing. This yields a virtually framed bracket polynomial distinct from the model in the previous section and to generalization of this model to an invariant,  $\overline{Z}(K)$ , of virtual regular isotopy depending on infinitely many variables. Section 7 discusses Vassiliev invariants, defines graphical finite type and proves that the weight systems are finite for the virtual Vassiliev invariants arising from the Jones polynomial. Section 8 is a discussion of open problems.

### 2. DEFINING VIRTUAL KNOTS AND LINKS

A classical knot [1] can be represented by a diagram. The diagram is a 4-regular plane graph with extra structure at its nodes. The extra structure is classically intended to indicate a way to embed a circle in three-dimensional space. The shadow of a projection of this embedding is the given plane graph. Thus we are all familiar with the usual convention for illustrating a crossing by omitting a bit of arc at the node of the plane graph. The bit omitted is understood to pass underneath the uninterrupted arc. See Figure 1.

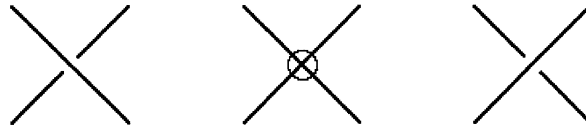


FIGURE 1. Crossings and virtual crossings.

From the point of view of a topologist, a knot diagram represents an ‘actual’ knotted (possibly unknotted) loop embedded in three space. The crossing structure is an artifact of the projection to the plane.

I shall define a virtual knot (or link) diagram. The definition of a virtual diagram is just this: we allow a new sort of crossing, denoted as shown in Figure 1 as a 4-valent vertex with a small circle around it. This sort of crossing is called virtual. It comes in only one flavor. You cannot switch over and under in a virtual crossing. However, the idea is not that a virtual crossing is just an ordinary graphical vertex. Rather, the idea is that the virtual crossing is not really there.

If I draw a non-planar graph in the plane, it necessarily acquires virtual crossings. These crossings are not part of the structure of the graph itself. They are artifacts of the drawing of the graph in the plane. The graph theorist often removes a crossing in the plane by making it into a knot theorist’s crossing, thereby indicating a particular embedding of the graph in three-dimensional space. This is just what we do not do with our virtual knot crossings, for then they would be indistinct from classical crossings. The virtual crossings are not there. We shall make sense of that property by the following axioms generalizing classical Reidemeister moves. See Figure 2.

The moves fall into three types: (a) classical Reidemeister moves relating classical crossings; (b) shadowed versions of Reidemeister moves relating only virtual crossings; and (c) a triangle move that relates two virtual crossings and one classical crossing.

The last move (type c) is the embodiment of our principle that the virtual crossings are not really there. Suppose that an arc is free of classical crossings. Then that arc can be arbitrarily moved (holding its endpoints fixed) to any new location. The new location will reveal a new set of virtual crossings if the arc that is moved is placed transversally to the remaining part of the diagram. See Figure 3 for illustrations of this process and for an example of unknotting of a virtual diagram.

The theory of virtual knots is constructed on this combinatorial basis—in terms of the generalized Reidemeister moves. We will make invariants of virtual knots by finding functions well defined on virtual diagrams that are unchanged under the application of the virtual moves. The remaining sections of this paper study many instances of such invariants.

### 3. MOTIVATIONS

While it is clear that one can make a formal generalization of knot theory in the manner so far described, it may not be yet clear why one should generalize in this particular way. This section explains two sources of motivation. The first is the study of knots in thickened surfaces of higher genus (classical knot theory is actually the theory of knots in a thickened two-sphere). The second is the extension of knot theory to the purely combinatorial domain of Gauss codes and Gauss diagrams. It is in this second domain that the full force of the virtual

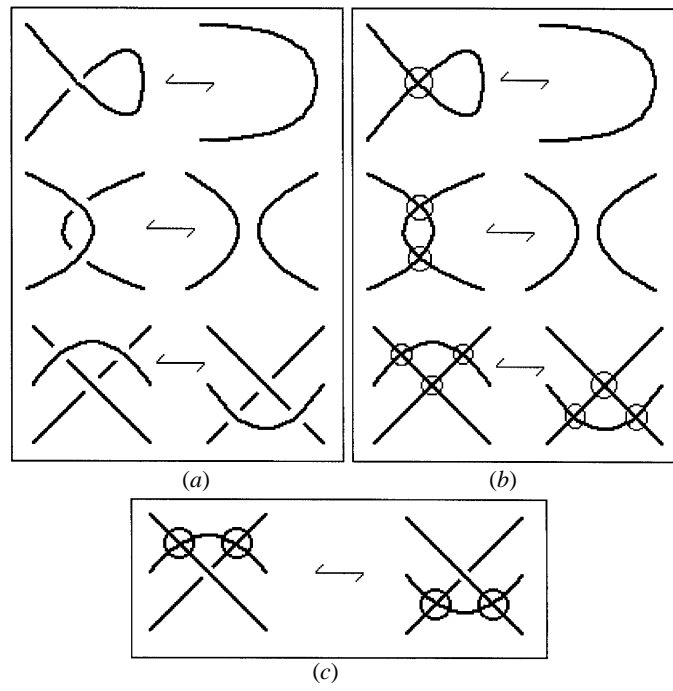


FIGURE 2. Generalized Reidemeister moves for virtual knot theory.

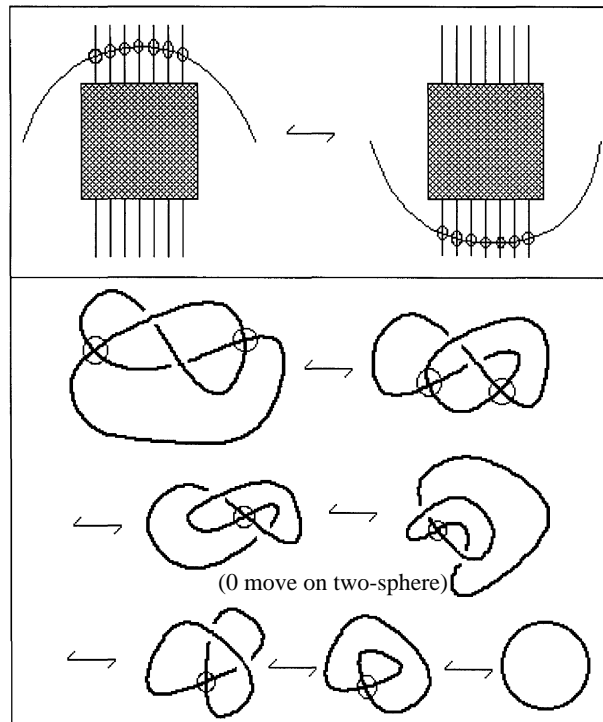


FIGURE 3. Virtual moves.

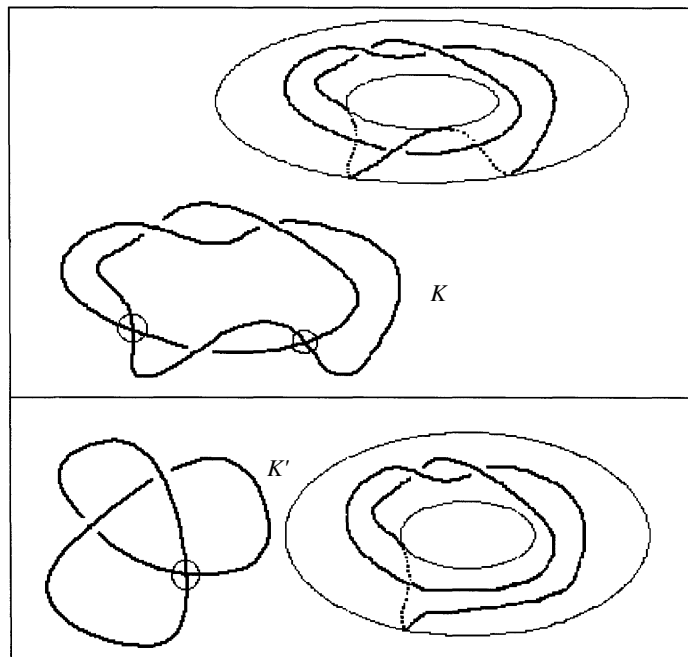


FIGURE 4. Two virtual knots.

theory comes into play.

*3.1. Surfaces.* Consider the two examples of virtual knots in Figure 4. We shall see later in this paper that these are both non-trivial knots in the virtual category. In Figure 4 we have also illustrated how these two diagrams can be drawn (as knot diagrams) on the surface of a torus. The virtual crossings are then seen as artifacts of the projection of the torus to the plane.

The knots drawn on the toral surface represent knots in the three manifold  $T \times I$  where  $I$  is the unit interval and  $T$  is the torus. If  $S_g$  is a surface of genus  $g$ , then the knot theory in  $S_g \times I$  is represented by diagrams drawn on  $S_g$  taken up to the usual Reidemeister moves transferred to diagrams on this surface.

As we shall see in the next section, abstract invariants of virtual knots can be interpreted as invariants for knots that are specifically embedded in  $S_g \times I$  for some genus  $g$ . The virtual knot theory does not demand the use of a particular surface embedding, but it does apply to such embeddings. This constitutes one of the motivations.

*3.2. Gauss codes.* A second motivation comes from the use of so-called *Gauss codes* to represent knots and links. The Gauss code is a sequence of labels for the crossings with each label repeated twice to indicate a walk along the diagram from a given starting point and returning to that point. In the case of multiple link components, we mean a sequence labels, each repeated twice and intersticed by partition symbols '/' to indicate the component circuits for the code.

A *shadow* is the projection of a knot or link on the plane with transverse self-crossings and no information about whether the crossings are overcrossings or undercrossings. In other words, a shadow is a 4-regular plane graph. On such a graph we can count circuits that always cross (i.e., they never use two adjacent edges in succession at a given vertex) at each

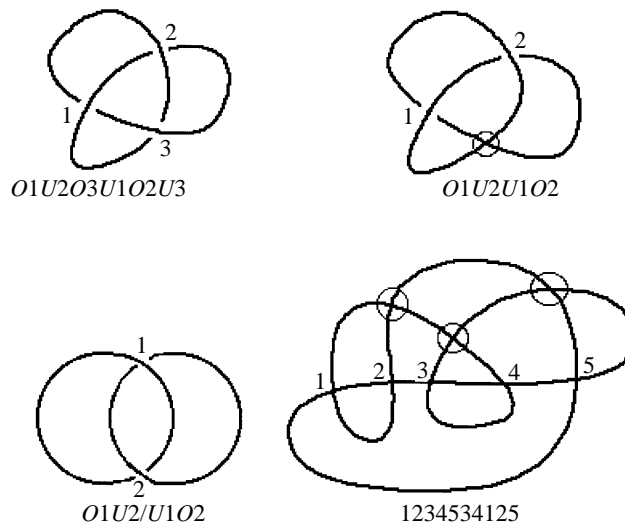


FIGURE 5. Planar and non-planar codes.

crossing that they touch. Such circuits will be called the *components* of the shadow since they correspond to the components of a link that projects to the shadow.

A single component shadow has a Gauss code that consists in a sequence of crossing labels, each repeated twice. Thus, the trefoil shadow has code 123123. A multi-component shadow has as many sequences as there are components. For example, 12/12 is the code for the Hopf link shadow.

Along with the labels for the crossings one can add the symbols *O* and *U* to indicate that the passage through the crossing was an overcrossing (*O*) or an undercrossing (*U*). Thus,

$$123123$$

is a Gauss code for the shadow of a trefoil knot and

$$O1U2O3U1O2U3$$

is a Gauss code for the trefoil knot. The Hopf link itself has the code *O1U2/U1O2*. See Figure 5.

Suppose that *g* is such a sequence of labels and that *g* is free of any partition labels. Every label in *g* appears twice. The first necessary criterion for the planarity of *g* is given by the following definition and Lemma.

DEFINITION. A single component Gauss code *g* is said to be *evenly intersticed* if there is an *even* number of labels in between the two appearances of any label.

LEMMA 1. *If g is a single component planar Gauss code, then g is evenly intersticed.*

PROOF. This follows directly from the Jordan curve theorem in the plane. □

EXAMPLE. The necessary condition for planarity in this Lemma is not sufficient. The code  $g = 1234534125$  is evenly intersticed but not planar as is evident from Figure 5.

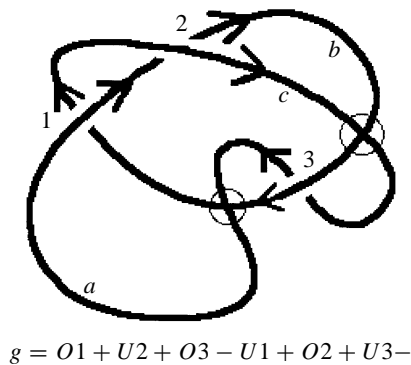


FIGURE 6. Signed Gauss codes.

Non-planar Gauss codes give rise to an infinite collection of virtual knots.

Local orientations at the crossings give rise to another phenomenon: virtual knots whose Gauss codes have planar realizations with different local orientations from their classical counterparts.

By orienting the knot, one can give orientation signs to each crossing relative to the starting point of the code—using the convention shown in Figure 6. This convention designates each oriented crossing with a *sign* of +1 or -1. We say that the crossing has positive sign if the overcrossing line can be turned through the smaller angle (of the two vertical angles at the crossing) to coincide with the direction of the undercrossing line. The signed code for the standard trefoil is

$$t = O1 + U2 + O3 + U1 + O2 + U3+,$$

while the signed code for a figure eight knot is

$$f = O1 + U2 + O3 - U4 - O2 + U1 + O4 - U3 - .$$

Here we have appended the signs to the corresponding labels in the code. Thus, crossing number 1 is positive in the figure eight knot, while crossing number 4 is negative. See Figure 6 for an illustration corresponding to these codes.

Now consider the effect of changing these signs. For example, let

$$g = O1 + U2 + O3 - U1 + O2 + U3 - .$$

Then  $g$  is a signed Gauss code and as Figure 6 illustrates, the corresponding diagram is forced to have virtual crossings in order to accommodate the change in orientation. The codes  $t$  and  $g$  have the same underlying (unsigned) Gauss code  $O1U2O3U1O2U3$ , but  $g$  corresponds to a virtual knot while  $t$  represents the classical trefoil.

Carrying this approach further, we *define* a virtual knot as an equivalence class of oriented Gauss codes under abstractly defined Reidemeister moves for these codes—with no mention of virtual crossings. The virtual crossings become artifacts of a planar representation of the virtual knot. The move sets of type (b) and (c) for virtuals are diagrammatic rules that make sure that this representation of the oriented Gauss codes is faithful. Note, in particular, that the move of type (c) does not alter the Gauss code. With this point of view, we see that the signed codes are knot theoretic analogues of the set of all graphs, and that the classical knot (diagrams) are the analogues of the planar graphs. This is the fundamental combinatorial motivation for our definitions of virtual knots and their equivalences.

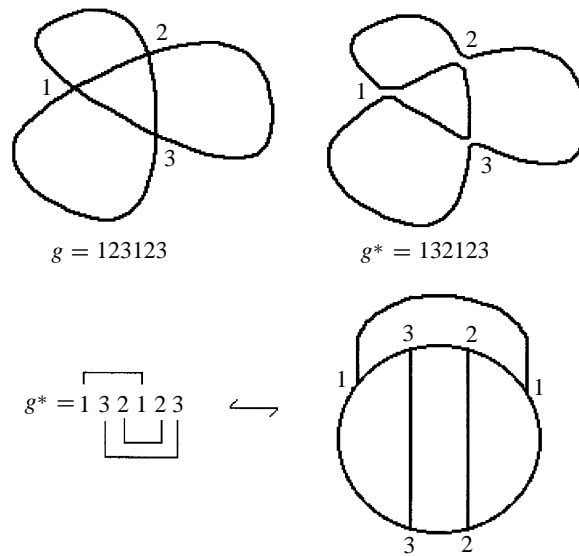


FIGURE 7. If  $g$  is planar, then  $g^*$  is dually paired.

Since it is useful to have a few more facts about the reconstruction of planar Gauss codes, we conclude this section with a quick review of that subject.

3.3. *Gauss codes and reconstruction.* In this section, we recall an algorithm for reconstructing a planar diagram from its Gauss code. This algorithm also detects non-planar codes. We shall see that for a planar oriented Gauss code, the orientation signs in the code sequence are determined up to a small number of choices. Such sign sequences will be called *standard* (with the more technical definition to follow).

We shall prove the following Theorem.

**THEOREM 2.** *If  $K$  is a virtual knot whose underlying Gauss code is planar and whose sign sequence is standard, then  $K$  is equivalent to a classical knot.*

The fundamental problem in Gauss codes is to provide an algorithm for determining whether a given code can be realized by a planar shadow.

We will explain the detection and reconstruction algorithms for single component codes. The first necessary condition for planarity for a single component code is that it be evenly intersticed, as we have already remarked in Lemma 1.

If a code  $g$  is planar, then a corresponding code for such an evenly paired Jordan curve can be produced as follows: let the labels in  $g$  be  $1, 2, \dots, n$ . Starting with  $i = 1$ , reverse the order of labels in between the two appearances of  $i$ . Do this successively using  $i = 1, 2, \dots, n$ . Let  $g^*$  be the resulting code.

In Figure 7 we see that the crossings of a planar shadow  $E$  can be smoothed to obtain a single Jordan curve in the plane. This Jordan curve can be seen as a circle with doubly repeated labels around its circumference so that some labels are paired by arcs inside the circle, and the remaining labels are paired by arcs outside the circle. The corresponding code is  $g^*$  as defined above. In this form of pairing, no two pairing arcs intersect one another.

**REMARK.** In the case of multiple component codes, the algorithm for constructing  $g^*$  is

modified as follows: suppose that the two appearances of  $i$  occur in different components of the code, so that the code to be modified has the form

$$h = i\alpha/i\beta/R,$$

where we have written the two components as adjacent code segments and started each with  $i$  (possible by rearrangement and cyclic permutation of the segments). Here  $R$  denotes the rest of the code sequences. Then replace  $h$  by

$$h' = i\alpha\bar{i}\bar{\beta}/R,$$

where  $\bar{\beta}$  denotes the rewrite of  $\beta$  in reverse order. Note that the two components are amalgamated into one as a result of this process. Thus, after applying this procedure successively to the labels in the code, we obtain a single code sequence  $g^*$  from a given multi-component code sequence  $g$ . For example, if  $g = 1234/1536/2546$ , then we obtain the following sequence of partial codes on the way to  $g^*$ :

$$\begin{aligned} g &= 1234/1536/2546 & g' &= 12341635/2546 = 23416351/2546 \\ g'' &= 234163512645 & g''' &= 236143512645 \\ g'''' &= 236146215345 & g''''' &= 236146215435 \\ g^* &= 236416215435. \end{aligned}$$

We leave it for the reader to check that  $g^*$  is dually paired.

We have the Lemma below.

LEMMA 3. *If  $g$  is a planar Gauss code, then  $g^*$  is dually paired.*

PROOF. The (easy) proof is omitted. See [3]. □

Figure 7 illustrates this situation and shows how the desired pairing can be written directly on the code  $g^*$  by pairing labels above and below the typographical line.

LEMMA 4. *If an evenly intersticed Gauss code  $g$  has  $g^*$  dually paired, then  $g$  is the Gauss code of a planar shadow.*

PROOF. Figure 8 shows how to reconstruct a shadow from any  $g$  satisfying the hypotheses of the Lemma. □

These lemmas form the essentials of the reconstruction theory for planar Gauss codes.

DEFINITION. A Gauss code  $g$  is said to be *prime* if it cannot be written as the juxtaposition of two Gauss codes on disjoint collections of labels. A non-prime code is said to be *composite*. For example, 123123 is prime but 121234543 is composite since it is the juxtaposition of 1212 and 34543.

In reconstructing a shadow from a Gauss code, there is a choice of local orientation of the first crossing in the code. From then on, the local orientations are determined by the reconstruction algorithm. See Figure 8 for an example of the procedure. Once we specify the local orientations in the code, the corresponding signs of the crossings are determined by whether there is an  $O$  or a  $U$  in the code. Thus up to these initial choices of orientation, the signs in an  $O/U$  code are all determined if the code is planar. It is this result that gives the proof of Theorem 2.

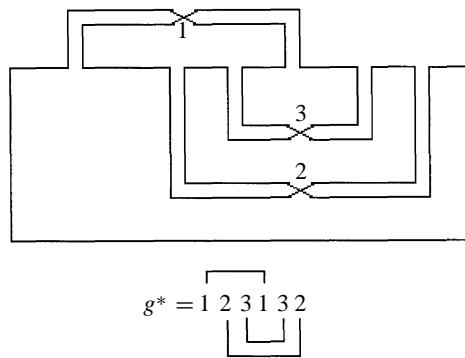


FIGURE 8. Reconstruction from a Gauss code.

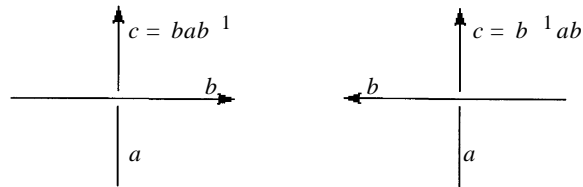


FIGURE 9. Generators and relations for the fundamental group.

PROOF OF THEOREM 2. Note that the reconstruction algorithm will give a planar embedding for this code with the same local orientations as those specified in the virtual diagram. In fact, we can assume that the planar positions of the crossings in the embedded diagram and the virtual diagram are identical (up to a global translation if comparison is desired). Now locate those arcs in the original diagram that involve virtual crossings and move them one-by-one into the positions indicated by the embedding. To accomplish this, start at the beginning of the code. Say the code reads  $g = a_1 a_2 \dots a_i a_{i+1} \dots a_n$ . In the virtual diagram, there may be a series of virtual crossings between  $a_1$  and  $a_2$  but there will be no real crossings since the code is given by  $g$ . Therefore, the arc from  $a_1$  to  $a_2$  can be replaced (by virtual equivalence) to its position in the embedded diagram. Continue this process sequentially for  $a_i a_{i+1}$  and the result is an equivalence through the virtual category of the original diagram with the embedded classical diagram. This completes the proof of Theorem 2.  $\square$

#### 4. FUNDAMENTAL GROUP, CRYSTALS, RACKS AND QUANDLES

The fundamental group of the complement of a classical knot can be described by generators and relations, with one generator for each arc in the diagram and one relation for each crossing. The relation at a crossing depends upon the type of the crossing and is either of the form  $c = b^{-1}ab$  or  $c = bab^{-1}$  as shown in Figure 9.

We define the group  $G(K)$  of an oriented virtual knot or link by this same scheme of generators and relations. An *arc* of a virtual diagram proceeds from one classical undercrossing to another (possibly the same) classical undercrossing. Thus no new generators or relations are added at a virtual crossing. It is easy to see that  $G(K)$  is invariant under all the moves for virtuals and hence is an invariant of virtual knots.

There are virtual knots that are non-trivial but have a trivial fundamental group. (We say

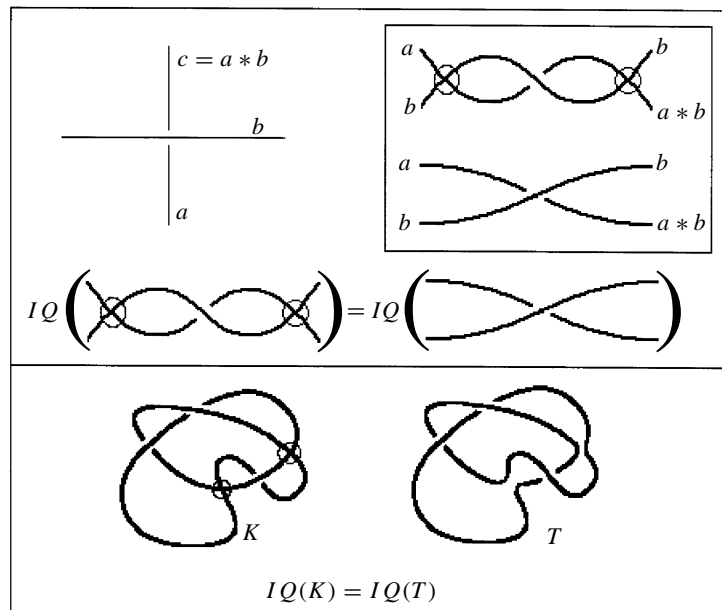


FIGURE 10. The involutory quandle.

that the fundamental group of a knot is trivial if it is isomorphic to the infinite cyclic group.) The virtual  $K'$  in Figure 4 is such an example. We shall show that  $K'$  is a non-trivial virtual in the next section by using a generalization of the bracket polynomial.

A generalization of the fundamental group called the quandle, rack or crystal (depending on notations and history) also assigns relations (in a different algebra) to each crossing. The quandle generalizes to the virtual category. We first discuss the involutory quandle,  $IQ(K)$ , for a (virtual) knot or link  $K$ . The  $IQ(K)$  does not depend upon the local orientations of the diagram and it assigns to each crossing the relation  $c = a * b$  as in Figure 10.

The operation  $a * b$  is a non-associative binary operation on the underlying set of the quandle, and it satisfies the following axioms:

- (1)  $a * a = a$  for all  $a$ .
- (2)  $(a * b) * b = a$  for all  $a$  and  $b$ .
- (3)  $(a * b) * c = (a * c) * (b * c)$  for all  $a, b, c$ .

The algebra under these axioms with generators and relations as defined above is called the involutory quandle,  $IQ(K)$ . It is easy to see that the  $IQ(K)$  is well-defined for  $K$  virtual.

An important special case of  $IQ(K)$  is the operation  $a * b = 2b - a$  where  $a$  and  $b$  are elements of a cyclic group  $Z/nZ$  for some modulus  $n$ . In the case of a knot  $K$ , there is a natural choice of modulus  $D(K) = \text{Det}(M(K))$  where  $M(K)$  is a minor of the matrix of relations associated with the set of equations  $c = 2b - a$ . This is called the determinant of the knot, in the classical case, and we shall call it the determinant of the virtual knot. If  $K$  is virtual, then  $|D(K)|$  is an invariant of  $K$ . The virtual knot labelled  $K$  in Figure 4 has a determinant equal to 3. The non-triviality of the determinant shows that this knot is knotted and, in fact, that it has non-trivial fundamental group.

Another example of an involutory quandle is the operation  $a * b = ba^{-1}b$ . In classical knot theory, this yields the fundamental group of the two-fold branched covering along the knot.

Here is a useful lemma concerning the  $IQ$  for virtuals.

LEMMA 5.

$$IQ(K_{v xv}) = IQ(K_{\bar{x}}),$$

where  $x$  denotes a crossing in the diagram  $K$ ,  $v xv$  denotes that  $x$  is flanked by virtuals, and  $K_{\bar{x}}$  denotes the diagram obtained by smoothing the flanking virtuals, and switching the intermediate crossing.

In other words, the  $IQ$  for a classical crossing flanked by two virtual crossings is the same as the  $IQ$  of the diagram where the two virtual crossings are smoothed and the classical crossing is switched.

PROOF. See Figure 10. □

REMARK. In Figure 10 we illustrate that  $IQ(K) = IQ(T)$  where  $K$  is the virtual knot also shown in Figure 6 and  $T$  is the trefoil knot.

Finally, we discuss the full quandle of a knot and its generalization to virtuals. For this discussion, the exponential notation of Fenn and Rourke [4] is convenient. Instead of  $a * b$ , we write  $a^b$  and assume that there is an operation of order two

$$a \longrightarrow \bar{a},$$

so that

$$\bar{\bar{a}} = a,$$

and for all  $a$  and  $b$

$$\overline{a^b} = \bar{a}^b.$$

This operation is well defined for all  $a$  in the underlying set  $Q$  of the quandle.

By definition

$$a^{bc} = (a^b)^c$$

for all  $a, b$  and  $c$  in  $Q$ .

The operation of exponentiation satisfies the axioms:

- (1)  $a^a = a$ .
- (2)  $a^{b\bar{b}} = a$ .
- (3)  $a^{(b^c)} = a^{\bar{c}bc}$ .

It follows that the set of the quandle acts on itself by automorphisms

$$x \longrightarrow x^a.$$

This group of automorphisms is a representation of the fundamental group of the knot. Note that if we define  $a^b$  by the formula

$$a^b = bab^{-1}$$

and

$$\bar{b} = b^{-1},$$

then we obtain the fundamental group itself as an example of a quandle. The rack [4] or crystal [5] is obtained by eliminating the first axiom. This makes the rack/crystal an invariant of

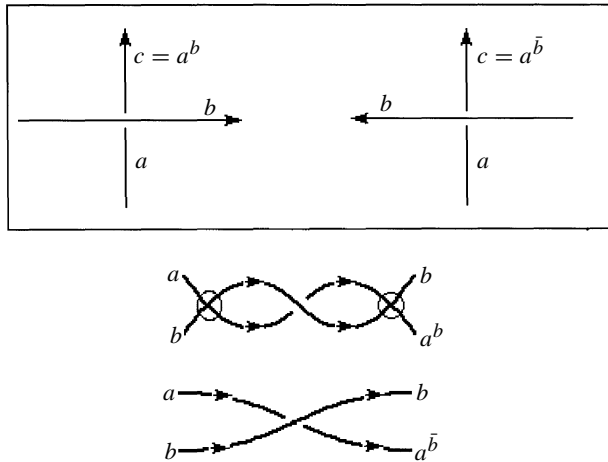


FIGURE 11. Change of relations for the full quandle.

framed knots and links. The three axioms correspond to invariance under the three Reidemeister moves.

If we now compare Lemma 5 with its possible counterpart for the full fundamental group or the quandle, we see that it no longer holds. Figure 11 shows the new relations in the quandle that are obtained after smoothing the two virtual crossings and switching the classical crossing. While the quandle of the simplified diagram is no longer isomorphic to the original quandle, the fact that we can articulate the change is often useful in computations.

EXAMPLE. Consider the virtual knot  $K$  of Figure 6. We have seen that  $K$  has the same  $IQ$  as the trefoil knot. However, the quandle and fundamental group of  $K$  are distinct from those of the trefoil knot, and  $K$  is not equivalent to any classical knot. To see this, consider the *Alexander quandle* [5] defined by the equations

$$a^b = ta + (1 - t)b$$

and

$$a^{\bar{b}} = t^{-1}a + (1 - t^{-1})b.$$

This quandle describes a module (the Alexander module)  $M$  over  $Z[t, t^{-1}]$ . In the case of the virtual knot  $K$  in Figure 6, we have the generating quandle relations  $a^c = b, b^a = c, c^{\bar{b}} = a$ . This results in the Alexander module relations  $b = ta + (1 - t)c, c = tb + (1 - t)a, a = t^{-1}c + (1 - t^{-1})b$ . From this, it is easy to calculate that the module  $M(K) = \{0, m, 2m\}$  for a non-zero element  $m$  with  $3m = 0$  and  $tm = 2m$ . Thus, the Alexander module for  $K$  is cyclic of order three. Since no classical knot has a finite cyclic Alexander module, this proves that  $K$  is not isotopic through virtuals to a classical knot.

Finally, it should be remarked that the full quandle  $Q(K)$  classifies a classical prime unoriented knot  $K$  up to mirror images. By keeping track of a *longitude* for the knot, one obtains a complete classification. In the context of the quandle, the longitude can be described as the automorphism

$$\lambda : Q(K) \longrightarrow Q(K)$$

defined by the formula

$$\lambda(x) = x^{a_1^{\epsilon_1} a_2^{\epsilon_2} \dots a_k^{\epsilon_k}},$$

where  $\{a_1, a_2, \dots, a_k\}$  is an ordered list of quandle generators encountered (as one crosses underneath) as overcrossing arcs as one takes a trip around the diagram. The  $\epsilon$  denotes whether the generator is encountered with positive or negative orientation, and  $x^\epsilon$  denotes  $x$  if  $\epsilon = 1$  and  $\bar{x}$  if  $\epsilon = -1$ . For a given diagram, the longitude is well defined up to cyclic re-ordering of this list of encounters. Exactly the same definition applies to virtual knots. It is no longer true that the quandle plus longitude classifies a virtual knot, as our examples of knotted virtuals with a trivial fundamental group show.

On the other hand, we can use the quandle to prove the following result. This proof is due to Goussarov, Polyak and Viro [9].

**THEOREM 6.** *If  $K$  and  $K'$  are classical knot diagrams such that  $K$  and  $K'$  are equivalent under extended virtual Reidemeister moves, then  $K$  and  $K'$  are equivalent under classical Reidemeister moves.*

**PROOF.** Note that longitudes are preserved under virtual moves (adding virtual crossings to the diagram does not change the expression for a longitude). Thus, an isomorphism from  $Q(K)$  to  $Q(K')$  induced by extended moves preserves longitudes. Since the isomorphism class of the quandle plus longitudes classifies classical knots, we conclude that  $K$  and  $K'$  are classically equivalent. This completes the proof.  $\square$

**REMARK.** We would like to see a purely combinatorial proof of Theorem 6.

**4.1. The GPV example and a generalization.** We end this section with a variation of an example [6, 9] that shows that it is possible to have a virtual knot  $K$  with  $Q(K)$  not isomorphic with  $Q(K^*)$  where  $K^*$  is the mirror image of  $K$ . In other words, there are *two* quandles, or two fundamental groups associated with any given virtual knot!

This example is a slightly different take on an observation in [9]. Let  $K$  be a given (virtual) diagram, drawn in the plane. Pick the diagram up and turn it over (note that the crossings change diagrammatically, but correspond to the result of physically turning over the layout of criss-crossing strands with welds at the virtual crossings). Let  $Flip(K)$  denote this overturned diagram. Define a new quandle  $Q^*(K)$  by the formula  $Q^*(K) = Q(Flip(K))$ . Goussarov, Polyak and Viro take their ‘other’ fundamental group to be the one defined by generators and relations obtained by ‘looking at the knot from the other side of the plane’. At the quandle level this is the same as taking  $Q^*(K)$ . It is easy to see that  $Q^*(K)$  is isomorphic to  $Q(K^*)$ . (Just note that if  $c = a^{\bar{b}}$ , then  $\bar{c} = \overline{a^{\bar{b}}} = \bar{a}^{\bar{b}}$ . Use this to check that the two quandles are isomorphic through the mapping  $a \rightarrow \bar{a}$  taking one to the other.) Thus our version of this example is mathematically equivalent to the GPV version.

In Figure 12, the reader will find  $K$  and  $K^*$  with labelled arcs  $a, b, c, d$ . In  $K$ , the quandle relations are  $a = b^d, b = c^d, c = d^b, d = a^b$ . The three-coloring of  $K$  in  $Z/3Z$  with  $a = 0, b = 2, c = 0, d = 1$  demonstrates that this quandle, and hence the fundamental group of  $K$ , is non-trivial. On the other hand,  $K^*$  has quandle relations  $a = a^a, c = b^c, d = c^c, a = d^a$ , giving a trivial quandle. Thus  $K$  is distinguished from  $K^*$  by the quandle. This example also shows that  $K$  has a non-trivial Alexander polynomial (using the fundamental group to define the Alexander polynomial—there is more than one Alexander polynomial for virtuals) but  $K^*$  has an Alexander polynomial equal to 1.

We generalize this example by considering the 1–1 tangle  $W$  shown in Figure 13. Replacing a straight arc in a knot diagram by  $W$  does not affect the quandle, while replacing by its

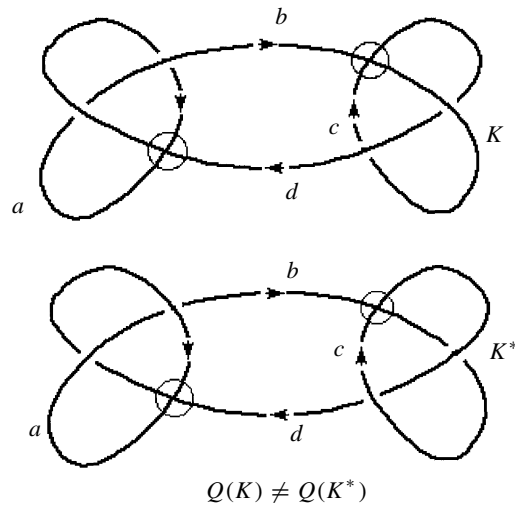


FIGURE 12.  $Q(K)$  is distinct from  $Q(K^*)$ .

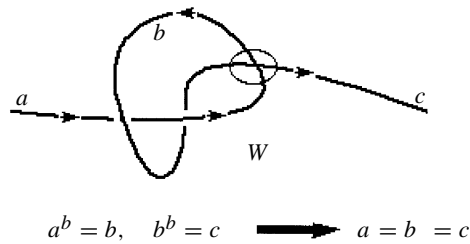


FIGURE 13. The 1-1 tangle  $W$ .

mirror image  $W^*$  changes the quandle relations in a generally non-trivial way (as in the GPV example). Insertion of  $W$  into knot diagrams produces infinitely many examples of pairs of virtual knots with the same quandle but different Jones polynomials. This last statement will be verified in the next section.

### 5. BRACKET POLYNOMIAL AND JONES POLYNOMIAL

The bracket polynomial [7] extends to virtual knots and links by relying on the usual formula for the state sum of the bracket, but allowing the closed loops in the state to have virtual intersections. Each loop is still valued at  $d = -A^2 - A^{-2}$  and the expansion formula

$$\langle K \rangle = A \langle K_a \rangle + A^{-1} \langle K_b \rangle$$

still holds where  $K_a$  and  $K_b$  denote the result of replacing a single crossing in  $K$  by smoothings of type  $a$  and type  $b$  as illustrated in Figure 14.

We must check that this version of the bracket polynomial is invariant under all but the first Reidemeister move (see the moves shown in Figure 2). Certainly, the usual arguments apply to the moves of type (a). Moves of type (b) do not disturb the loop counts and so leave bracket

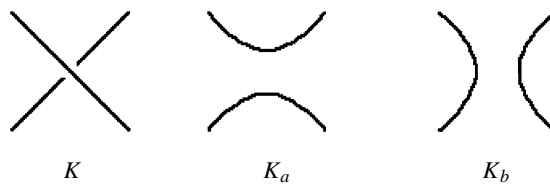


FIGURE 14. Bracket smoothings.

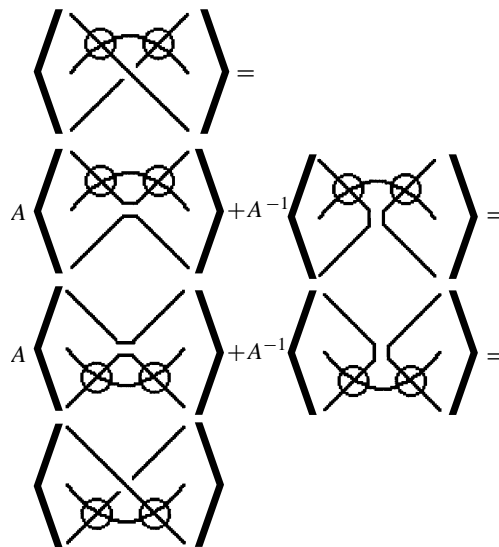


FIGURE 15. Type (c) invariance of the bracket.

invariant. Finally, the move of type (c) receives the verification illustrated in Figure 15. This completes the proof of the invariance of the generalized bracket polynomial under move (c).

We define the writhe  $w(K)$  for an oriented virtual to be the sum of the crossing signs—just as in the classical case.

The  $f$ -polynomial is defined by the formula

$$f_K(A) = (-A^3)^{-w(K)} \langle K \rangle(A).$$

The Laurent polynomial,  $f_K(A)$ , is invariant under all the virtual moves including the classical move of type I.

REMARK. It is worth noting that  $f_K$  can be given a state summation of its own. Here we modify the vertex weights of the bracket state sum to include a factor of  $-A^{-3}$  for each crossing of positive sign, and a factor of  $A^{+3}$  for each factor of negative sign. It is then easy to see that

$$f_{K_+} = -A^{-2} f_{K_0} - A^{-4} f_{K_\infty}, \quad f_{K_-} = -A^{+2} f_{K_0} - A^{+4} f_{K_\infty},$$

where  $K_+$  denotes  $K$  with a selected positive crossing,  $K_-$  denotes the result of switching only this crossing,  $K_0$  denotes the result of making the oriented smoothing of this crossing,

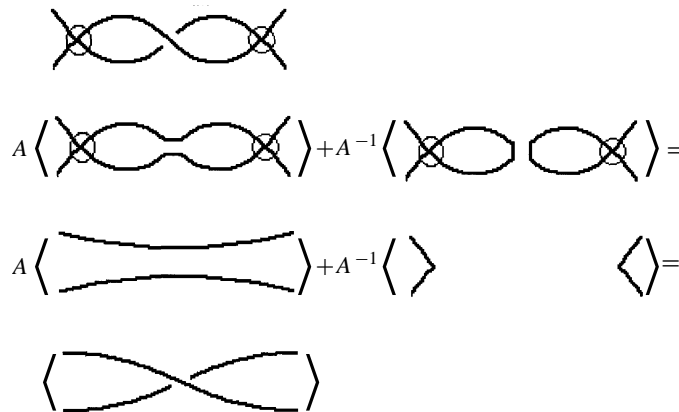


FIGURE 16. Removal of flanking virtual crossings.

and  $K_\infty$  denotes the result of making an unoriented smoothing at this crossing. The states in this oriented state sum acquire sites with unoriented smoothings, but the procedure for evaluation is the same as before. For each state we take the product of the vertex weights multiplied by  $d^{\|S\|-1}$  where  $d = -A^2 - A^{-2}$  and  $\|S\|$  denotes the number of loops in the state. Then  $f_K$  is the sum of these products, one for each state.

The following Lemma makes virtual calculations easier.

LEMMA 7.  $\langle K_{v_x v} \rangle = \langle K_x \rangle$  where  $x$  denotes a crossing in the diagram  $K$ ,  $v_x v$  denotes that  $x$  is flanked by virtuals and  $K_x$  denotes the diagram obtained by smoothing the flanking virtuals and leaving the crossing the same.

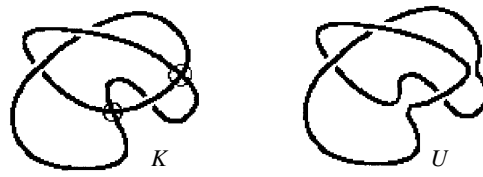
PROOF. The proof is shown in Figure 16. □

Note that this result has the opposite form from our corresponding lemma concerning the involutory quandle  $IQ(K)$ . As a result we obtain an example of a virtual knot that is non-trivial (via the  $IQ$ ) but has  $f_K = 1$ . Hence we have a virtual knot  $K$  with a Jones polynomial equal to 1. The example is shown in Figure 17. Note that in Figure 10 we illustrated that this  $K$  has the same involutory quandle as the trefoil knot. We saw in Section 4 that  $K$  is not equivalent to a classical knot.

We now compute the bracket polynomial for our previous example with a trivial fundamental group and we find that  $\langle K' \rangle = A^2 + 1 - A^{-4}$  and  $f_{K'} = (-A^3)^{-2} \langle K' \rangle = A^{-4} + A^{-6} - A^{-10}$ . Thus  $K'$  has a non-trivial Jones polynomial. See Figure 18.

In Figure 18, we also indicate the result of placing the tangle  $W$ , discussed in Figure 13, into another knot or link. Since this is the same as taking a connected sum with  $K'$ , it has the effect of multiplying the bracket polynomial by  $A^2 + 1 - A^{-4}$ . Thus, if  $L$  is any knot or link and  $K' + L$  denotes the connected sum of  $K'$  along some component of  $L$ , then  $\langle K' + L \rangle = (A^2 + 1 - A^{-4}) \langle L \rangle$  while  $Q(K' + L) = Q(L)$  (as we verified in the last section). Thus for any knot  $L$ , successive connected sums with  $K'$  produces an infinite family of distinct virtual knots, all having the same quandle (hence the same fundamental group).

Finally, we note that if the knot is given as embedded in  $S_g \times I$  for a surface of genus  $g$ , and if its virtual knot diagram  $K$  is obtained by projecting the diagram on  $S_g$  into the plane, then



$$\langle K \rangle = \langle U \rangle = -A^3$$

FIGURE 17. A knotted virtual with a trivial Jones polynomial.

$\langle K \rangle$  computes the value of the extension of the bracket to the knots in  $S_g \times I$  where all the loops have the same value  $d = -A^2 - A^{-2}$ . This is the first-order bracket for link diagrams on a surface.

In Figure 4 we illustrated the non-trivial knot  $K$  with a trivial Jones polynomial as embedded in  $S_1 \times I$ . This knot in  $S_1 \times I$  is actually not trivial as can be seen from the higher Jones polynomials that discriminate loops in different isotopy classes on the surface.

In Figure 19 is another example of a virtual knot  $E$  and a corresponding embedding in  $S_1 \times I$ . In this case,  $E$  is a trivial virtual knot (as is shown in Figure 3), but the embedding of  $E$  in  $S_1 \times I$  is non-trivial (even though it has a trivial fundamental group and trivial bracket polynomial). The non-triviality of this embedding is seen by simply observing that it carries a non-trivial first homology class in the thickened torus. In fact, if you expand the state sum for the bracket polynomial and keep track of the isotopy classes of the curves in the states, then the bracket calculation also shows this non-triviality by exhibiting as its value a single state with a non-contractible curve.

Virtual knot theory provides a convenient calculus for working with knots in  $S_g \times I$ . The virtuals carry many properties of knots in  $S_g \times I$  that are independent of the choice of embedding and genus. This completes our quick survey of the properties of the bracket polynomial and Jones polynomial for virtual knots and links. Just as uncolorable graphs appear when one goes beyond the plane (for planar graph coloring problems), so knots of unit Jones polynomial appear as we leave the diagrammatic plane into the realm of the Gauss codes.

## 6. QUANTUM LINK INVARIANTS

There are virtual link invariants corresponding to every quantum link invariant of classical links. However, this must be said with a caveat: we do not assume invariance under the first classical Reidemeister move (hence these are invariants of regular isotopy) and we do not assume invariance under the flat version of the first Reidemeister move in the (b) list of virtual moves. Otherwise, the usual tensor or state sum formulas for quantum link invariants extend to this generalized notion of regular isotopy invariants of virtual knots and links. In this section, we illustrate this method by taking a different generalization of the bracket that includes virtual framing. We apply this new invariant to distinguish a virtual knot that has Jones polynomial equal to one and a trivial fundamental group.

In order to carry out this program, we quickly recall how to construct quantum link invariants in the unoriented case. See [5] for more details. The link diagram is arranged with respect to a given ‘vertical’ direction in the plane so that perpendicular lines to this direction intersect the diagram transversely or tangentially at maxima and minima. In this way, the diagram can be seen as constructed from a pattern of interconnected maxima, minima and crossings—as

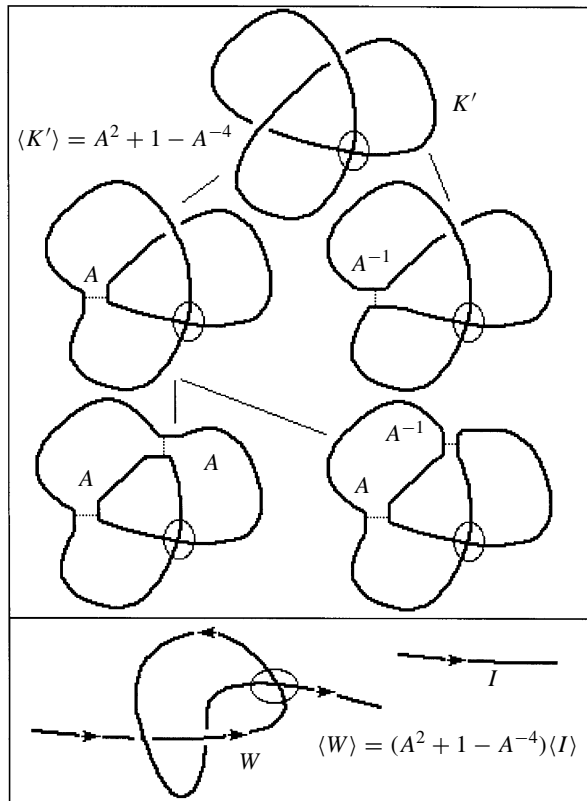


FIGURE 18. Calculation of  $\langle K' \rangle$ .

illustrated in Figure 20.

As illustrated in Figure 20, we associate the symbols  $M_{ab}$  and  $M^{ab}$  to minima and maxima, respectively, and the symbols  $R_{cd}^{ab}$  and  $\bar{R}_{cd}^{ab}$  to the two types of crossings. The indices on these symbols indicate how they are interconnected. Each maximum or minimum has two lines available for connection corresponding to the indices  $a$  and  $b$ . Each  $R, \bar{R}$  has four lines available for connection. Thus, the symbol sequence

$$T(K) = M_{ad}M_{bc}M^{ek}M^{lh}R_{ef}^{ab}R_{gh}^{cd}\bar{R}_{kl}^{fg}$$

represents the trefoil knot as shown in Figure 20. Since repeated indices show the places of connection, there is no necessary order for this sequence of symbols. I call  $T(K)$  an *abstract tensor expression* for the trefoil knot  $K$ .

By taking matrices (with entries in a commutative ring) for the  $M$ s and the  $R$ s, it is possible to re-interpret the abstract tensor expression as a summation of products of matrix entries over all possible choices of indices in the expression. Appropriate choices of matrices give rise to link invariants. If  $K$  is a knot or link and  $T(K)$  its associated tensor expression, let  $Z(K)$  denote the evaluation of the tensor expression that corresponds to the above choice of matrices. We will assume that the matrices have been chosen so that  $Z(K)$  is an invariant of regular isotopy.

The generalization of the quantum link invariant  $Z(K)$  to virtual knots and links is quite straightforward. We simply ignore the virtual crossings in the diagram. Another way to put

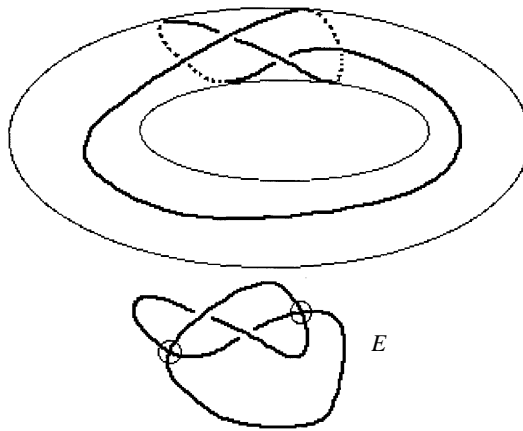


FIGURE 19. A knot in  $S_1 \times I$  with a trivial Jones polynomial.

this is that we take each virtual crossing to be represented by crossed Kronecker deltas as in Figure 20. The virtual crossing is represented by the tensor

$$V_{cd}^{ab} = \delta_d^a \delta_c^b.$$

Here,  $\delta_b^a$  is the Kronecker delta. It is equal to 1 if  $a = b$  and is equal to 0 otherwise. (Note that the Kronecker delta is well defined as an abstract tensor.)

In extending  $Z(K)$  to virtual knots and links by this method, we cannot hope to obtain invariance under the type I virtual move. In fact, as Figure 20 shows, the presence of a virtual curl is indexed by the transpose  $M_{ba}$  of the tensor  $M_{ab}$ . Thus we define *virtual regular isotopy* to be invariance under all the extended Reidemeister moves for virtuals except type (a)I and (b)I. It is easy to see that  $Z(K)$  extends in this way when  $Z(K)$  is an invariant of regular isotopy for classical links.

In particular, the bracket polynomial for classical knots is obtained by letting the indices run over the set  $\{1, 2\}$  with  $M^{ab} = M_{ab}$  for all  $a$  and  $b$  and  $M_{11} = M_{22} = 0$  while  $M_{12} = iA$  and  $M_{21} = -iA^{-1}$  where  $i^2 = -1$ . The  $R$ s are defined by the equations

$$\begin{aligned} R_{cd}^{ab} &= AM^{ab}M_{cd} + A^{-1}\delta_c^a\delta_d^b, \\ \overline{R}_{cd}^{ab} &= A^{-1}M^{ab}M_{cd} + A\delta_c^a\delta_d^b. \end{aligned}$$

These equations for the  $R$ s are the algebraic translation of the smoothing identities for the bracket polynomial. Then we have:

**THEOREM 8.** *With  $Z(K)$  defined as above and  $K$  a classical knot or link,  $Z(K) = d(K)$  where  $d = -A^2 - A^{-2}$ .*

**PROOF.** See [5]. □

For this extension of  $Z(K)$  to virtuals, there is a state summation similar to that of the bracket polynomial. For this, let  $C$  be a diagram in the plane that has only virtual crossings. View this diagram as an immersion of a circle in the plane. Let  $\text{rot}(C)$  denote the absolute value of the Whitney degree of  $C$  as a immersion in the plane. (Since  $C$  is unoriented, only the absolute value of the Whitney degree is well-defined.) The Whitney degree of an oriented

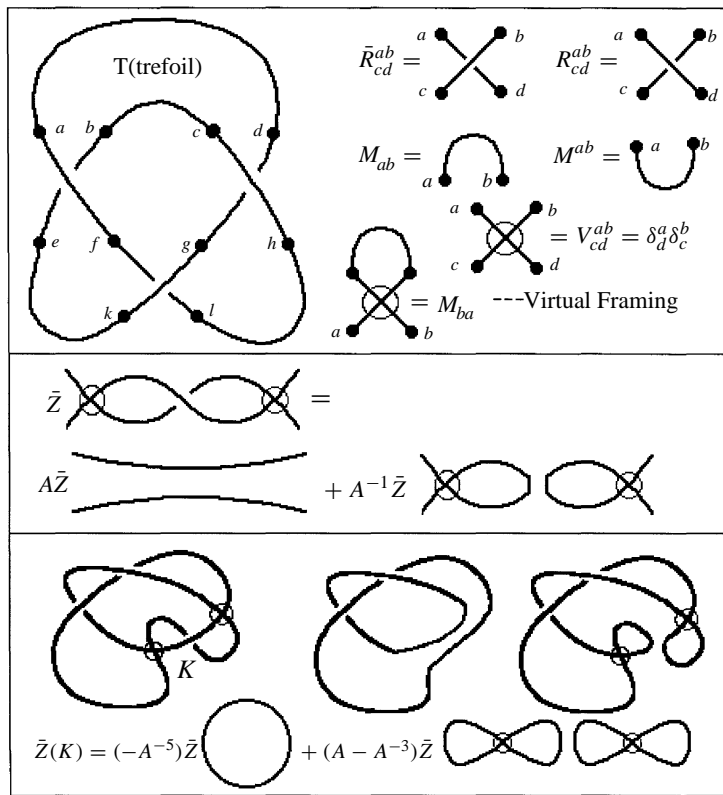


FIGURE 20. Quantum link invariants.

plane immersion is the total algebraic number of  $2\pi$  turns of the unit tangent vector to the curve as the curve is traversed once. Let  $d(C)$  be defined by the equation

$$d(C) = (-1)^{\text{rot}(C)}(A^{2\text{rot}(C)} + A^{-2\text{rot}(C)}).$$

Let  $S$  be a state of a virtual diagram  $K$  obtained by smoothing each classical crossing in  $K$ . Let  $C \in S$  mean that  $C$  is one of the curves in  $S$ . Let  $\langle K|S \rangle$  denote the usual product of vertex weights ( $A$  or  $A^{-1}$ ) in the bracket state sum. Then:

PROPOSITION 9. *The invariant of virtual regular isotopy  $Z(K)$  is described by the following state summation:*

$$Z(K) = \sum_S \langle K|S \rangle \prod_{C \in S} d(C),$$

where the terms in this formula are as defined above. Note that  $Z(K)$  reduces to  $d(K)$  when  $K$  is a classical diagram.

PROOF. The proof is a calculation based on the tensor model explained in this section. The details of this calculation are omitted.  $\square$

REMARK. The state sum in Proposition 9 generalizes to an invariant of virtual regular isotopy with an infinite number of polynomial variables, one for each regular homotopy

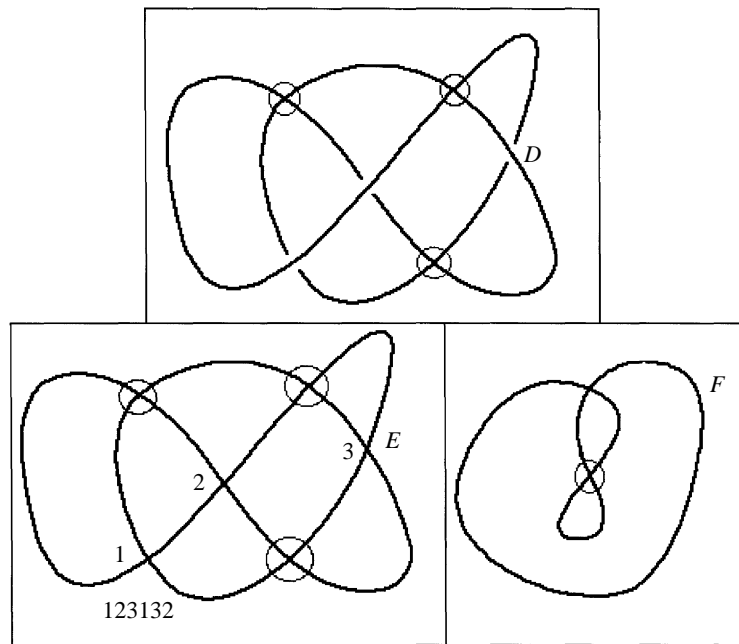


FIGURE 21.  $D$  has unit a Jones polynomial and trivial fundamental group.

class of unoriented curve immersed in the plane. To make this generalization, let  $A_n$  for  $n = 0, 1, 2, 3, \dots$  denote a denumerable set of commuting independent variables. If  $C$  is an immersed curve in the plane, define  $\text{Var}(C) = A_n$  where  $n = \text{rot}(C)$ , the absolute value of the Whitney degree of  $C$ . We take  $A_1 = -A^2 - A^{-2}$  as before, but the other variables are independent of each other and of  $A$ .

Now define the generalization of  $Z(K)$ , denoted  $\bar{Z}(K)$ , by the formula

$$\bar{Z}(K) = \sum_S \langle K|S \rangle \prod_{C \in S} \text{Var}(C).$$

In this definition, we have replaced the evaluation  $d(C)$  by the corresponding variable  $\text{Var}(C)$ . In Figure 20 we illustrate the result of calculating  $\bar{Z}(K)$  for a knot  $K$  with a unit Jones polynomial. The result is

$$\bar{Z}(K) = (-A^{-5})A_1 + (A - A^{-3})A_0^2.$$

Since the coefficients of  $A_1$  and  $A_0$  are themselves invariants of virtual regular isotopy, it follows, as we already knew, that  $K$  is a non-trivial virtual. This non-triviality is detected by our refinement  $\bar{Z}(K)$  of the bracket polynomial. A similar phenomenon of refinement of invariants happens with other quantum link invariants. This will be the subject of a separate paper.

We end this section with an application of Proposition 9. Let  $D$  be the virtual knot diagram shown in Figure 21.

It is easy to see that  $D$  has an  $f$ -polynomial equal to 1, and hence a Jones polynomial equal to 1. Use Lemma 7 to show that  $\langle D \rangle = -A^3$ .  $D$  also has a trivial fundamental group and

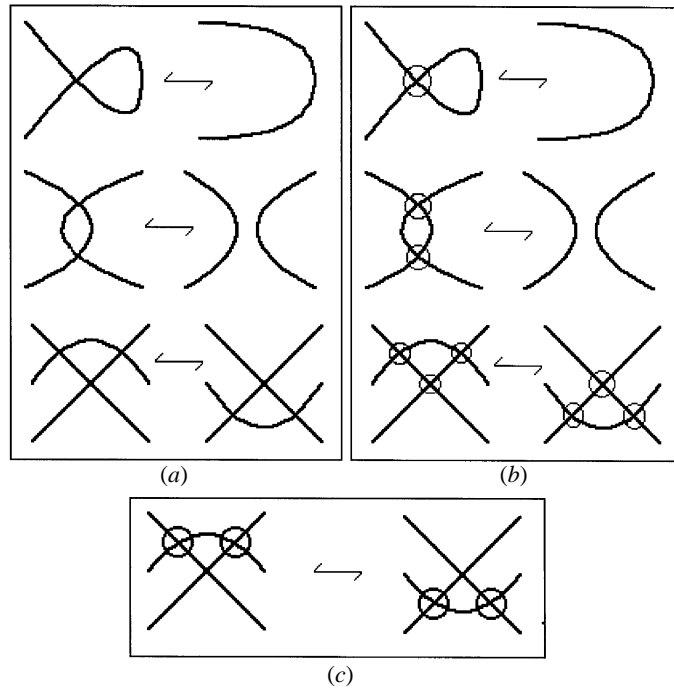


FIGURE 22. Flat virtual moves.

quandle. Is  $D$  a non-trivial virtual knot? The answer is yes! It follows from the calculation of  $Z(D)$ . We omit the calculation, but give the result

$$Z(D) = A^7 - A^5 - 4A^3 + 2A + A^{-1} - A^{-3}.$$

It follows from this that  $D$  cannot be regularly isotopic to a standard virtual curl form. Hence  $D$  must be virtually knotted in the regular isotopy category. On the other hand, I do not yet have a proof that  $D$  is virtually knotted under the original definition that allows the addition and removal of virtual framings. This example shows both the power and limitation of using the quantum invariants to study virtual knots.

There should be a direct way to see that  $D$  is knotted. Let  $E$  denote the *shadow* of the diagram  $D$ . That is, replace the classical crossings in  $D$  with flat crossings. Regard the flat crossings as *distinct* from virtual crossings, so that we obtain the rules for virtual isotopy of flat diagrams shown in Figure 22. By these rules, a flat diagram corresponds to an oriented Gauss code without over- or undercrossing specifications. The virtual moves preserve the Gauss code just as before.

$E$  is illustrated in Figure 21. Is  $E$  flat virtually equivalent to a circle with curls and virtual curls? I conjecture that the answer is no. Simpler examples of this sort of irreducibility are easy to produce. The diagram  $F$  in Figure 21 is irreducible because  $Z(F)(1) = -2A_0 + A_2$ , as is easy to compute.

These examples lead us to the following definition. We call the *shadow code* of a diagram the underlying Gauss code of that diagram without any specifications of orientation or over/under-crossing. We say that a virtual diagram is *almost classical* if its shadow code is planar.

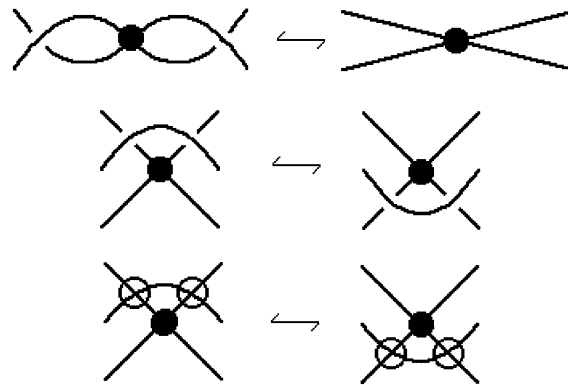


FIGURE 23. Moves for rigid vertex embeddings.

CONJECTURE. There does not exist a non-trivial almost classical virtual knot with both a trivial fundamental group and trivial Jones polynomial.

## 7. VIRTUAL VASSILIEV INVARIANTS

We now study embeddings into  $R^3$  (Euclidean three-space) of 4-valent graphs up to *rigid vertex isotopy*. In rigid vertex isotopy, one can think of each graphical vertex as a rigid disk. The four graphical edges incident to this vertex are attached to the boundary of the disk at four specific points. In a rigid vertex isotopy, the embedded edges of the graph can be isotoped freely, but the disks must move without deformation in the course of the isotopy. A consequence of this definition [8] is that the diagrammatic moves shown in Figure 23 capture rigid vertex isotopy just as the Reidemeister moves capture ambient isotopy. Figure 23 shows only the move types that are added to the usual list of Reidemeister moves. Two graphs with diagrammatic projections  $G_1$  and  $G_2$  are rigid vertex isotopic if and only if there is a series of moves of this type joining the two diagrams.

In Figure 23 there is also illustrated the one addition to virtual moves that is needed to complete the move set for rigid vertex isotopy of virtual knotted graphs. In this addition, an arc with consecutive virtual crossings is moved to a new position across a rigid vertex. Here we must make a distinction between the graphical rigid vertices and the virtual vertices in the diagrams. Once this is done, we directly extend discussions of invariants of rigid vertex graphs to invariants of virtual rigid vertex graphs. To see how this is done we will discuss invariants obtained by insertion into the vertices of a graph. We shall always mean the extension to virtual equivalence when we refer to ambient isotopy or to rigid vertex isotopy.

If one replaces each node of a (virtual) rigid vertex graph  $G$  with a tangle (possibly virtual) to form a virtual link  $K$ , then any rigid equivalence of  $G$  induces a corresponding equivalence of  $K$ . The consequence of this remark is that we can obtain invariants of rigid vertex graphs from any invariant of (virtual) knots and links by taking a systematic choice of tangle insertion. That is, if we have chosen tangle insertions  $T_1, \dots, T_n$ , let  $\{v_1, \dots, v_m\}$  denote the set of vertices of  $G$  and let  $a = (a_1, \dots, a_m)$  with  $1 \leq a_i \leq n$  denote a choice of tangle insertion for each vertex of  $G$ . Then let  $G^a$  denote the result of inserting tangle  $T_{a_i}$  at node  $i$  in  $G$ . Suppose that  $R(K)$  is an ambient isotopy invariant of virtual knots and links  $K$ . Then define

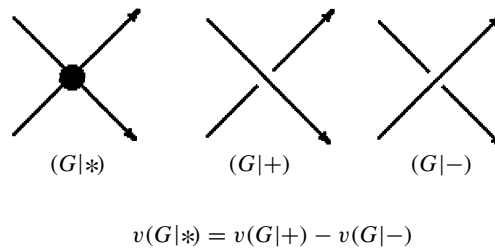


FIGURE 24. Vassiliev invariant identity.

an extension of  $R$  to graphical imbeddings by the formula

$$R(G) = \sum_a x_{a_1} \dots x_{a_m} R(G^a),$$

where  $\{x_j | j = 1, \dots, m\}$  is a new set of variables (or constants) independent of the variables already present in the invariant  $R$ . Our discussion shows that  $R(G)$  is an invariant of virtual graph embeddings  $G$ .

While it is of interest to explore this larger class of induced invariants, we shall restrict ourselves to the generalization of *Vassiliev invariants*. A Vassiliev invariant  $v$  is an invariant of rigid vertex (virtual) 4-valent graphs that satisfies

$$v(G|*) = v(G|+) - v(G|-),$$

where  $(G|*)$  denotes an oriented graph  $G$  with a chosen vertex  $*$ .  $(G|+)$  denotes the result of replacing the vertex  $*$  with a positive crossing and  $(G|-)$  is the result of replacing it with a negative crossing. See Figure 24. This is the traditional definition of a Vassiliev invariant and we adopt it verbatim for virtuals.

DEFINITION. Let  $N(G)$  denote the number of vertices in the 4-valent graph  $G$ . A Vassiliev invariant  $v$  is said to be of *graphical finite type  $n$*  if  $v(G) = 0$  whenever  $N(G) > n$ . Note that this definition says nothing about the number of virtual crossings in the graph  $G$ .

Useful examples of virtual invariants of graphical finite type are obtained by taking the coefficients of  $x^m$  in

$$F_K(x) = f_K(e^x),$$

where  $F_K(x)$  is extended to 4-valent graphs by the difference formula

$$F_K(x)(G|*) = F_K(x)(G|+) - F_K(x)(G|-).$$

The corresponding formula then holds for the coefficients of  $x^m$  in the power series expansion of  $F_K(x)$ .

LEMMA 10. Let  $F_K(x) = f_K(e^x)$  denote the power series resulting from substitution of  $e^x$  for the variable  $A$  in the Laurent polynomial  $f_K(A)$  (defined in Section 2). Write this power series in the form

$$F_K(x) = \sum_{m=0}^{\infty} v_m(K)x^m.$$

Then the numerical invariants  $v_k(K)$  are of finite graphical type  $k$ .

PROOF. Recall from Section 5 that

$$\begin{aligned} f_{K_+} &= -A^{-2} f_{K_0} - A^{-4} f_{K_\infty}, \\ f_{K_-} &= -A^{+2} f_{K_0} - A^{+4} f_{K_\infty}. \end{aligned}$$

It follows that

$$\begin{aligned} F_{K_*} &= F_{K_+} - F_{K_-} \\ &= f_{K_+}(e^x) - f_{K_-}(e^x) \end{aligned}$$

is divisible by  $x$ . Thus, if  $G$  has  $m$  nodes, then  $F_G$  is divisible by  $x^m$ . This implies, for any  $G$ , that  $v_k(G) = 0$  if  $k < m = N(G)$ . This is exactly the statement that  $v_k$  is of finite graphical type  $k$ .  $\square$

PROPOSITION 11. *Let  $G$  be a graph with  $n$  vertices so that  $N(G) = n$ , configured as a virtual diagram in the plane. Let  $(G|+)$  denote the diagram  $G$  with a specific crossing of positive type and  $(G|-)$  the diagram identical to  $G$  except that the crossing has been switched to one of negative type. Let  $(G|*)$  denote the result of replacing this crossing by a graphical vertex. Let  $v$  be a Vassiliev invariant of type  $n = N(G)$ . Then  $v(G|+) = v(G|-)$ . Thus, a Vassiliev invariant of type  $n$  is independent of the settings of the crossings (plus or minus) in a diagram for  $G$ .*

PROOF.  $v(G|+) - v(G|-) = v(G|*)$  by the definition of a Vassiliev invariant. But  $v(G|*) = 0$  since  $(G|*)$  has  $(n + 1)$  vertices and  $v$  is of type  $n$ . This completes the proof.  $\square$

COROLLARY 12. *If  $G$  and  $v$  are as in Proposition 11, and  $G$  is a classical diagram (free of virtual crossings), then  $v(G)$  does not depend upon the classical embedding of  $G$  in  $R^3$  that is indicated by the diagram.*

PROOF. This follows directly from the switching independence shown in Proposition 11.  $\square$

For virtual Vassiliev invariants, one should not expect the analog of this corollary to hold, but in fact it does hold for the virtual Vassiliev invariants induced from  $f_K(A)$ . That is, we shall show that the Vassiliev invariants  $v_n(G)$  in the series  $F_K(x)$  depend only on the chord diagram associated with  $G$  when  $G$  is a virtual diagram with  $n$  graphical nodes. This is the subject of the following subsection.

7.1. *The Vassiliev invariants induced by the Jones polynomial.* We shall use the Vassiliev invariants that arise from the bracket polynomial and the  $f$ -polynomial. This is equivalent to using the Vassiliev invariants that arise from the Jones polynomial. Let  $f(A)$  be any Laurent polynomial with coefficients as in the formula below

$$f(A) = c_1 A^{d_1} + c_2 A^{d_2} + \dots + c_k A^{d_k},$$

where the degrees are integers arranged so that

$$d_1 \leq d_2 \leq \dots \leq d_k.$$

Then

$$\begin{aligned} f(e^x) &= c_1 e^{x d_1} + c_2 e^{x d_2} + \cdots + c_k e^{x d_k} \\ &= \sum_{n=0}^{\infty} (c_1 d_1^n + c_2 d_2^n + \cdots + c_k d_k^n) x^n / n!. \end{aligned}$$

Thus, if

$$F(x) = f(e^x) = \sum_{n=0}^{\infty} v_n x^n,$$

then

$$v_n = (c_1 d_1^n + c_2 d_2^n + \cdots + c_k d_k^n) / n!.$$

This gives a direct formula for the Vassiliev invariants  $v_n$  associated with  $f$ .

In particular, this gives us a direct method to read off the Vassiliev invariants associated with a given evaluation of the normalized bracket polynomial  $f_K$ . The invariant  $v_n(G)$  is determined by the coefficients of  $f_G(A)$  and the exponents of  $A$  in this Laurent polynomial.

NOTATIONAL DISCUSSION. Let  $v_n(K)$  denote the  $n$ th Vassiliev invariant induced from  $f_K(A)$  as described in this section. Let  $G_*$ ,  $G_+$ ,  $G_-$  denote a triple of (virtual) graph diagrams that differ at the site of one rigid vertex (denoted  $*$ ) by replacement by either a positive crossing (denoted  $+$ ) or a negative crossing (denoted  $-$ ). Let  $G_0$  and  $G_\infty$  denote the oriented and unoriented smoothings of this crossing. Note that since we can speak of the evaluation of  $f_{G_\infty}(A)$ , it follows that  $v_n$  is defined for diagrams with non-oriented smoothings—one just evaluates the state sum in the usual way with single reverse-oriented loops taking the usual loop value of  $-A^2 - A^{-2}$ .

THEOREM 13. *With notation as above, the following recursion formula holds for the Vassiliev invariants  $v_n(G)$ .*

$$v_n(G_*) = \sum_{k=0}^{n-1} c_{n,k} (v_k(G_0) + 2^{n-k} v_k(G_\infty)),$$

where

$$(2^{n-k} (1 + (-1)^{n-k+1}) / (n-k)!) = c_{n,k}.$$

The value of  $v_0(K)$  on a virtual diagram without graphical nodes depends only on the number of components in the diagram, and is independent of the configuration of virtual crossings. Specifically,

$$v_0(K) = (-2)^{\mu(K)-1},$$

where  $\mu(K)$  denotes the number of link components in  $K$ .

COROLLARY 14. *The Vassiliev invariants  $v_n(G)$  in the series  $F_K(x)$  depend only on the chord diagram associated with  $G$  when  $G$  is a virtual diagram with  $n$  graphical nodes. Hence, the weight systems for the invariants  $v_n(G)$  do not depend upon virtual crossings.*

PROOF OF COROLLARY 14. This follows directly from Theorem 13 since the recursion formula in that theorem computes  $v_n(G)$  for a graph  $G$  with  $n$  nodes in terms of  $v_0(K)$  for a collection of virtual knots  $\{K\}$ . Since  $v_0$  is independent of virtual crossings, so is  $v_n(G)$ . This completes the proof.  $\square$

PROOF OF THEOREM 13. Recall from Section 5 that

$$\begin{aligned} f_{G_+} &= -A^{-2}f_{G_0} - A^{-4}f_{G_\infty}, \\ f_{G_-} &= -A^{+2}f_{G_0} - A^{+4}f_{G_\infty}. \end{aligned}$$

Hence,

$$f_{G_*} = (A^2 - A^{-2})f_{G_0} + (A^4 - A^{-4})f_{G_\infty}.$$

Now suppose that

$$f_{G_0} = \sum_i a_i A^{n_i}$$

and that

$$f_{G_\infty} = \sum_i b_i A^{m_i}.$$

Then,

$$f_{G_*} = \sum_i a_i A^{n_i+2} - a_i A^{n_i-2} + b_i A^{m_i+4} - b_i A^{m_i-4}.$$

Therefore

$$v_n(G_*) = (1/n!) \sum_i a_i ((n_i + 2)^n - (n_i - 2)^n) + b_i ((m_i + 4)^n - (m_i - 4)^n).$$

The first part of Theorem 13 follows from this formula by a direct application of the binomial theorem. For the second part, note that

$$v_0(K) = f_K(1) = (-1)^{w(K)} \langle K \rangle(1).$$

For  $A = 1$ , it is easy to see that the only effect of the matrix model of Section 6 on the bracket calculation is to multiply it by  $(-1)^{cv(K)}$  where  $cv(K)$  is the number of virtual crossings in  $K$ . That is,

$$d \langle K \rangle(1) = (-1)^{cv(K)} Z(K)(1),$$

where  $Z(K)(1)$  is the matrix model of Section 6 evaluated at  $A = 1$ .

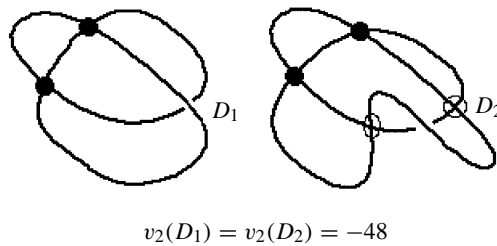
In this matrix model, there is no difference (at  $A = 1$ ) between the crossings and the virtual crossings. They are both algebraically crossed Kronecker deltas. Consequently,  $Z(K) = Z(K')$  where  $K'$  is the same diagram as  $K$  with all the virtual crossings replaced by (flat) classical crossings. Then it follows from the regular isotopy invariance of  $Z$  that  $Z(K')(1) = (-2)^{\mu(K)} (-1)^{c(K')}$  where  $c(K')$  is the total number of crossings in  $K'$ . Note that the value of  $d = -2$  when  $A = 1$ . Hence

$$v_0(K) = (-1)^{w(K)} (-1)^{cv(K)} (-1)^{c(K')} (-2)^{\mu(K)-1}.$$

Now we know that  $w(K) + cv(K)$  is congruent modulo 2 to  $c(K')$ . Therefore

$$v_0(K) = (-2)^{\mu(K)-1}.$$

This completes the proof of the theorem. □

FIGURE 25.  $v_2$  dependence.

REMARK. An example for this theorem is that  $v_2$  gives the value  $-48$  for both of the graphs shown in Figure 25. Each graph has two graphical nodes. One graph represents a virtual diagram inequivalent to any embedding of the other. The invariants  $v_n(G)$  themselves depend on virtual crossings for the graphs with less than  $n$  nodes. In fact, in these intermediate ranges, there is a dependency on infinitely many virtual diagrams, so that these invariants are no longer as ‘finite’ as the classical Vassiliev invariants. In [9] there is formulated a more restrictive notion of finite-type virtual invariants. Our  $v_2$  from the Jones polynomial is a first example of a finite-graphical-type invariant that is outside the scheme proposed by Goussarov, Polyak and Viro. More work needs to be done to have a complete theory of virtual Vassiliev invariants.

## 8. DISCUSSION

This completes our introduction to virtual knot theory. There is much that begs for further investigation. We leave the following topics for sequels to this paper: the Alexander polynomial (there are a diversity of definitions that differ on virtual knots), virtual braids, virtual three-manifolds, Vassiliev invariants induced from quantum link invariants, more general structure of Vassiliev invariants.

It should be remarked that the usual argument that induces Vassiliev invariants from quantum link invariants produces virtual Vassiliev invariants from our natural extension of quantum link invariants. Of course, we have to handle the virtual framing for these cases as was discussed in Section 6. The matter of the virtual framing needs further thought since introducing it means that we are no longer just considering abstract Gauss codes.

For general Vassiliev invariants, it is worth comparing our results with those of Goussarov, Polyak and Viro [9]. The general notion of finite graphical type given here and their notion of finite type suggest a unification not yet fully perceived.

Virtual braids is a subject very close to the ‘welded braids’ of Fenn, Rimanyi and Rourke [10]. In fact, their welded braids are a quotient of the category of virtual braids that are defined through our approach. I am indebted to Tom Imbo for pointing out this connection. This topic will be the subject of a separate paper.

This work began with an attempt to understand the Jones polynomial for classical knots by generalizing that category. I hope that these considerations will lead to deeper insight into the Jones polynomial and its relationship with the fundamental group and quandle of a classical knot.

## ACKNOWLEDGEMENT

It gives the author pleasure to thank the National Science Foundation for support of this research under NSF Grant DMS-9205277, the NSA for partial support under grant No. MSPF-96G-179 and the Mittag-Leffler Institute for hospitality during the writing of this paper.

## REFERENCES

1. C. W. Ashley, *The Ashley Book of Knots*, Doubleday, New York, 1944.
2. L. H. Kauffman, Talks at: the MSRI Meeting in January 1997; AMS Meeting at the University of Maryland, College Park in March 1997; Isaac Newton Institute Lecture in November 1997; Knots in Hellas Meeting in Delphi, Greece in July 1998; APCTP-NANKAI Symposium on Yang-Baxter Systems, Non-Linear Models and Applications at Seoul, Korea in October 1998.
3. R. C. Read and P. Rosenstiehl, On the Gauss Crossing Problem, *Colloq. Math. Soc. Janos Bolyai*, **18**; *Combinatorics*, Keszthely, Hungary, (1976), 843–876.
4. R. Fenn and C. Rourke, Racks and links in codimension two, *J. Knot Theory Ram.*, **1** (1992), 343–406.
5. L. H. Kauffman, *Knots and Physics*, World Scientific, Singapore, 1991 and 1994.
6. O. Viro, Private conversation, 1998.
7. L. H. Kauffman, State models and the Jones polynomial, *Topology*, **26** (1987), 395–407.
8. L. H. Kauffman, *Knots and Diagrams*, Lectures at Knots '96, S. Suzuki (ed.), World Scientific, Singapore, 1997, pp. 123–194.
9. M. Goussarov, M. Polyak and O. Viro, Finite type invariants of classical and virtual knots, (preprint October 1998 – math.GT/9810073).
10. R. Fenn, R. Rimanyi and C. Rourke, The Braid permutation group, *Topology*, **36** (1997), 123–135.

LOUIS H. KAUFFMAN

*Department of Mathematics, Statistics and Computer Science,  
University of Illinois at Chicago,  
851 South Morgan Street,  
Chicago,  
IL 60607-7045, U.S.A.*